mechanical stretch up-regulates *brain natriuretic peptide (BNP)* gene expression through calcineurin and CaMKII.

2. Stretch induces gene expression in cultured cardiomyocytes

Mechanical stress has been considered to be one of the major stimuli that evoke hypertrophic responses including reprogramming of gene expression in cardiac myocytes (Komuro et al., 1990, 1991b; Komuro and Yazaki, 1993). To investigate the signaling pathways that translate mechanical stress into cardiac hypertrophy, we developed an in vitro device by which mechanical stress can be imposed on cardiac myocytes cultured in the serum-free condition. Prolonged stretch of neonatal rat cardiomyocytes cultured on an elastic silicone dish induces several hypertrophic responses such as activation of protein kinases (Yamazaki et al., 1993, 1995; Komuro et al., 1996; Pan et al., 1999), gene expression of immediate early genes or fetal type genes (Komuro et al., 1990, 1991b; Komuro and Yazaki, 1993; Sadoshima and Izumo, 1997), and an increase in protein synthesis (Mann et al., 1989). *BNP* has been reported to be up-regulated in the hypertrophied heart (Dagnino et al., 1992; Hanford et al., 1994), and Northern blot analysis reveals that *BNP* gene expression is strongly up-regulated by stretch (Fig. 1a).

3. Ca^{2+} is involved in stretch-induced gene expression

Since it has been recently demonstrated that Ca^{2+} acts as an important mediator for various hypertrophic stimuli (Frey et al., 2000), we examined whether Ca^{2+} is involved in stretch-induced *BNP* gene expression. Addition of a Ca^{2+} ionophore A23187 increased the expression levels of *BNP* in cardiac myocytes (Fig. 1b). Up-regulation of *BNP* gene expression was also induced by an increase in intracellular Ca^{2+} concentration following treatment with BayK8644, a calcium channel agonist, and thapsigargin (Thastrup et al., 1990), a sarcoplasmic reticulum (SR) calcium ATPase inhibitor (Fig. 1b). On the contrary, pretreatment with EGTA, an extracellular Ca^{2+} chelator, strongly inhibited stretch-induced *BNP* gene expression (Fig. 1b). It has been reported that long-term treatment of cardiac myocytes with thapsigargin causes depletion of Ca^{2+} in SR and decreases the intracellular Ca^{2+} transient (Kirby et al., 1992). Long exposure with thapsigargin also inhibits stretch-induced *BNP* gene expression (Fig. 1b).

Our results indicate that an increase in intracellular Ca^{2+} levels induced by Ca^{2+} ionophore, Ca^{2+} channel agonist, or the SR calcium ATPase inhibitor, was sufficient to activate *BNP* gene expression (Fig. 1b). Intracellular Ca^{2+} regulates the expression of other cardiac genes such as the *atrial natriuretic factor (ANF)* (Irons et al., 1992; McDonough and Glembotski, 1992) and the *β-type myosin heavy chain (β-MHC)* (Zhu et al., 2000). However, the mechanisms by which intracellular Ca^{2+} regulates gene expression are not completely understood. Chelation of extracellular Ca^{2+} with EGTA abolished stretch-induced *BNP* expression (Fig. 1b), suggesting that Ca^{2+} influx from extracellular space is necessary. Since depletion of Ca^{2+} in the SR suppressed the stretch-induced *BNP* gene up-regulation, a large increase in intracellular Ca^{2+} level accomplished by CICR may be necessary for gene induction.

4. Ion channels as mechanosensors

Stretch-induced *BNP* gene expression is also abolished by the treatment with stretch-activated ion channel inhibitors such as gadolinium and streptomycin (Ohmori, 1985; Yang and Sachs, 1989), or voltage-dependent Ca^{2+} channel antagonists such as nifedipine and amlodipine (Fig. 1b), suggesting that Ca^{2+} influx through voltage-dependent Ca^{2+} channels and possibly through stretch-activated ion channels may be involved in stretch-induced gene expression.

Ion channels and exchangers on the cell membrane have been postulated to be potential "mechano-receptors", because they may respond promptly to stretch and convert it into intracellular signals (Komuro and Yazaki, 1993). It was reported that mechanical stretch of cultured chick cardiac myocytes evokes calcium influx and subsequent CICR from the SR, which

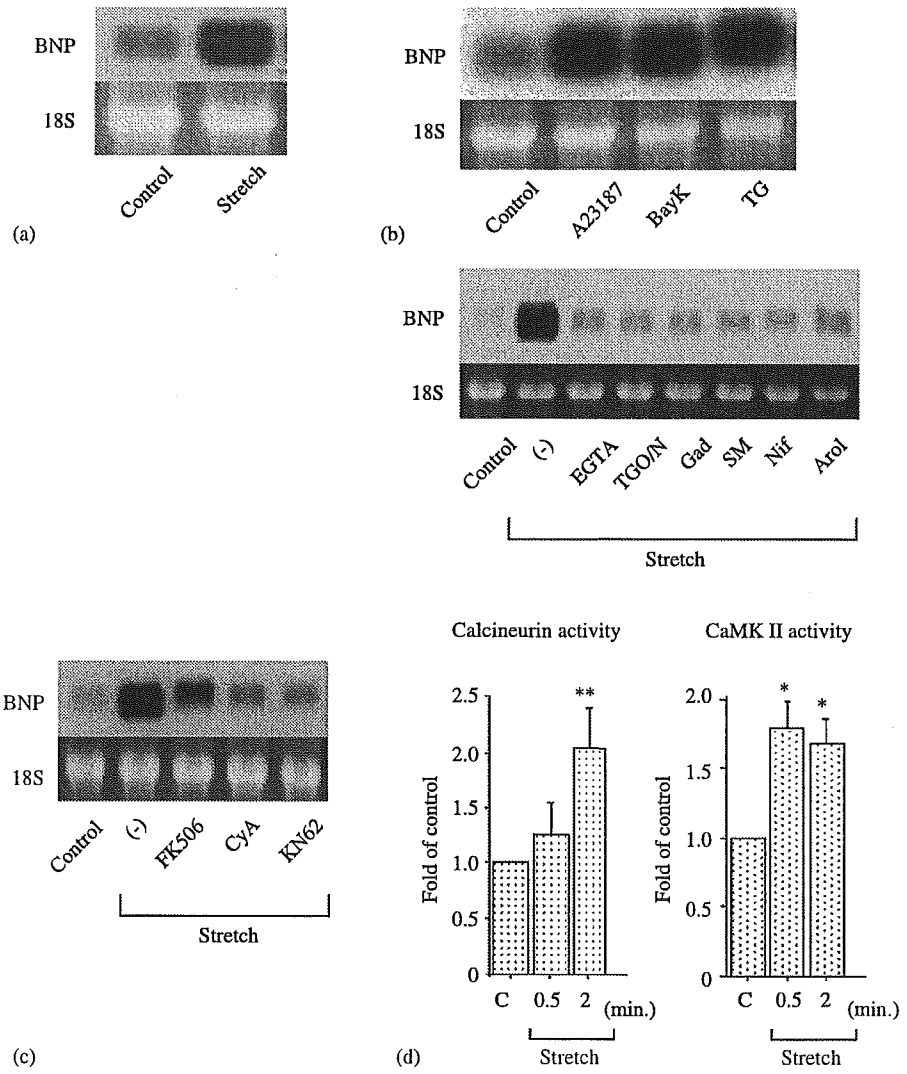

was abrogated by gadolinium (Sigurdson et al., 1992). Previously, we and others have reported that inhibitors of stretch-activated ion channels, such as gadolinium and streptomycin, do not block stretch-induced expression of *c-fos* (Komuro et al., 1991a; Sadoshima et al., 1992) and activation of MAP kinases (Yamazaki et al., 1998). Pan et al. reported that gadolinium and EGTA did not attenuate stretch-induced phosphorylation of *s*ignal *t*ransducers and *a*ctivators of *t*ranscription (STAT)1 and STAT3 (Pan et al., 1999). In our study, however, pretreatment of gadolinium and streptomycin significantly inhibited *BNP* gene expression induced by stretch (Fig. 1b). Although gadolinium and streptomycin are not specific to stretch-activated ion channels (Hu and Sachs, 1997), these results suggest that Ca^{2+} entry through stretch-activated ion channels may be involved in *BNP* gene expression, but not in expression of *c-fos* gene or activation of MAP kinases and Janus kinase/STAT pathway.

Voltage-dependent Ca^{2+} channel antagonists, nifedipine and amlodipine, significantly suppress *BNP* gene expression by mechanical stretch. Furthermore, Ruwhof et al. have reported that the voltage-dependent Ca^{2+} channel antagonist diltiazem blocks the stretch-induced increase in intracellular calcium levels by $\sim$50% in cardiomyocytes (Ruwhof et al., 2001), suggesting the following two possibilities; (1) activity of voltage-dependent Ca^{2+} channel is stretch-activated or (2) the inward current of cations through stretch-activated ion channels causes membrane depolarization which in turn opens the Ca^{2+} channels. Transgenic mice which overexpress voltage-dependent Ca^{2+} channel α1-subunit in the heart exhibit cardiac hypertrophy (Muth et al., 1999, 2001). Furthermore, we found that blocking of the voltage-dependent Ca^{2+} channels by continuous infusion of nifedipine was sufficient to suppress the activity of calcineurin and prevent the development of cardiac hypertrophy in spontaneously hypertensive rats (Zou et al., 2002). These results suggest that an increase in Ca^{2+} influx through the voltage-dependent Ca^{2+} channels are necessary for the generation of cardiac hypertrophy in vivo.

Na^{+}–H^{+} exchanger (NHE), another potential mechanosensitive ion exchnager, is activated by mechanical stretch (Cingolani et al., 1998). We have reported that pretreatment with an NHE

Fig. 1. Involvement of Ca^{2+} signaling in stretch-induced gene expression. (a) Mechanical stretch induces *BNP* gene expression. Cultured cardiac myocytes of neonatal rats were stretched by 20% for 30 min (stretch). *BNP* gene expression was examined by Northern blot analysis. 18S ribosomal RNA was stained with ethidium bromide, and used as a loading control. (b) Roles of Ca^{2+} in stretch-induced *BNP* gene expression. Cardiac myocytes were incubated with a Ca^{2+} ionophore A23187 (3 mM), a Ca^{2+} channel agonist BayK8644 (10 mM), or an SR calcium ATPase inhibitor thapsigargin (2 mM) for 30 min. Ca^{2+} influx and subsequent CICR are critically involved in stretch-induced *BNP* gene expression. On the contrary, pretreatment with an extracellular Ca^{2+} chelator EGTA (5 mM) strongly inhibited stretch-induced *BNP* expression. Pretreatment with inhibitors for stretch-activated ion channels, gadolinium (10 mM) or streptomycin (500 mM), and specific inhibitors for voltage-dependent Ca^{2+} channels nifedipine (1 mM) or amlodipine (1 mM), also attenuated stretch-induced *BNP* expression. Depleting Ca^{2+} store in SR by treatment with thapsigargin overnight inhibited stretch-induced *BNP* expression. SM, streptomycin; Nif, nifedipine; Amlo, amlodipine; TG, thapsigargin; TG O/N, treatment with thapsigargin overnight. (c) Calcineurin and CaMK are critically involved in stretch-induced *BNP* gene expression. Pretreatment with specific inhibitors for calcineurin FK506 (10 mM) and cyclosporin A (0.4 mM), and a specific inhibitor for CaMK KN62 (0.5 mM) significantly inhibited stretch-induced *BNP* expression. CyA, cyclosporin A. (d) Stretch increases the activity of calcineurin and CaMK in cultured cardiac myocytes. Cultured cardiac myocytes were stretched, and the activities of calcineurin and CaMK were determined by measuring the radioactivity of liberated ^{32}P from phosphorylated GST-RII and by assaying the phosphorylation of synthetic peptide autocamtide-2, respectively. Data were shown as mean $\pm$SE **, $p<0.01$ compared with control. *, $p<0.05$ compared with control. *C*, control.

inhibitor HOE694 inhibited stretch-induced activation of the protein kinase cascades and protein synthesis (Yamazaki et al., 1998). A rise in intracellular Na^+ may stimulates the reverse mode of the Na^+–Ca^{2+} exchanger (NCX) and causes increase in intracellular Ca^{2+}. In cat myocardium, stretch-induced increase in contractile force is attenuated by inhibition of either NHE or the reverse mode of NCX (Perez et al., 2001; Aiello et al., 2002). It remains unclear whether NHE and NCX are involved in stretch-induced activation of Ca^{2+} signaling and gene expression.

5. Role of calcineurin and CaMKII in stretch-induced gene expression

Increased intracellular Ca^{2+} binds to calmodulin and evokes a variety of events through Ca^{2+}/calmodulin-dependent enzymes such as calcineurin and CaMKs. Recently, the importance of these two pathways for the development of cardiac hypertrophy has been reported. Transgenic mice overexpressing constitutively activated mutant of calcineurin develop marked cardiac hypertrophy (Molkentin et al., 1998). Calcineurin inhibitors, FK506 (Shimoyama et al., 2000) and cyclosporin A (Meguro et al., 1999; Zhu et al., 2000; Zou et al., 2001a, b), inhibit AngII-, ET-1-, phenylephrine-, and isoproterenol-induced hypertrophic responses including *BNP* gene expression in cultured cardiac myocytes (Molkentin et al., 1998; Zhu et al., 2000). Furthermore, we and others have reported that calcineurin is critically involved in load- and agonist-induced cardiac hypertrophy in vivo (Sussman et al., 1998; Meguro et al., 1999; Shimoyama et al., 1999, 2000; Zou et al., 2001a, b). With regard to CaMK signaling, CaMKI and CaMKIV enhanced *ANF*- and *skeletal α-actin*-promoter activity, and transgenic mice overexpressing CaMKIV developed cardiac hypertrophy (Passier et al., 2000). Furthermore, the CaMKII inhibitor, KN62 (Zhu et al., 2000), prevented ET-1-induced hypertrophic responses such as expression of *β-MHC* and *ANF* genes, an increase in protein synthesis and induction of sarcomere organization (Irons et al., 1992; Zhu et al., 2000).

To elucidate the pathways downstream of Ca^{2+} involving stretch-induced gene expression, we examined the effects of specific inhibitors for these Ca^{2+}/calmodulin-dependent enzymes on stretch-induced *BNP* gene up-regulation. Pretreatment FK506 and cyclosporin A or a CaMKII inhibitor KN62 significantly inhibited stretch-induced *BNP* gene upregulation (Fig. 1c). We also found that calcineurin and CaMKII activities were increased by stretch (Fig. 1d), suggesting that both molecules may be involved in stretch-induced *BNP* gene expression.

6. Divergence of the signaling pathway in stretch-induced gene expression

Mechanical stretching of postnatal cardiomyocytes up-regulates expression of various kinds of genes, that are not typical fetal genes or natriuretic peptide genes. For example, myocardial stretch in an isolated rat heart model increases *vascular endothelial growth factor* (VEGF) expression (Li et al., 1997) by enhancing nuclear translocation of hypoxia-inducible factor-1 (HIF-1), which is a key transactivator of the *VEGF* gene under hypoxic conditions (Kim et al., 2002). Stretch-induced VEGF expression by HIF-1 is attenuated by gadolinium but not by diltiazem. In this model, phosphatidylinositol 3-kinase (PI3 K)-dependent Akt phosphorylation is activated by mechanical stretch, and a PI3 K inhibitor wortmannin suppressed up-regulation of

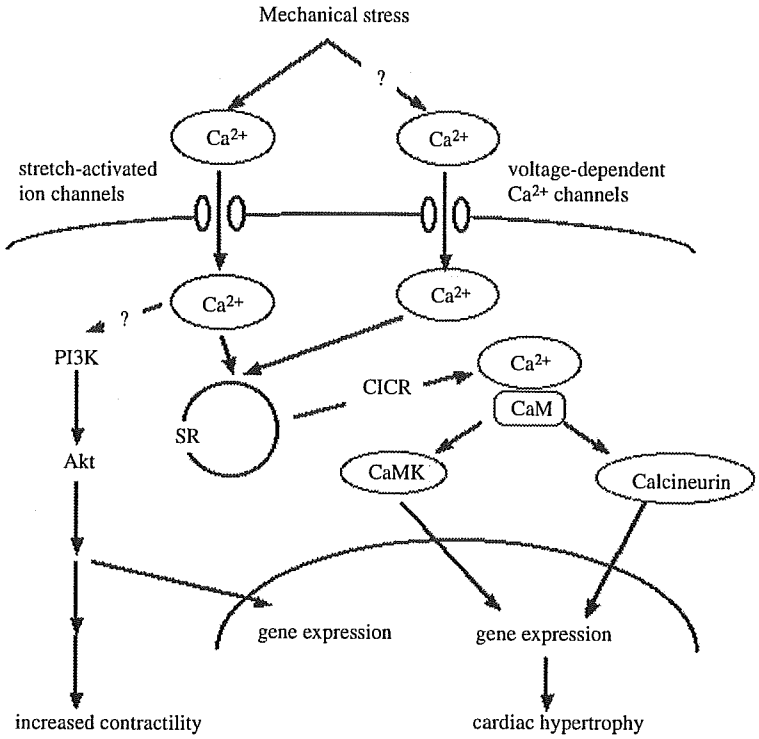

Fig. 2. Involvement of Ca^{2+} in mechanical stress-induced cardiac hypertrophy. Ca^{2+}/calmodulin-dependent enzymes are activated by calcium influx through ion channels and subsequent CICR, and play an important role in stretch-induced gene expression during the development of cardiac hypertrophy. Other pathways including the PI3K/Akt axis are involved in stretch-induced increase in myocardial contractility and gene expression.

the *VEGF* gene. These result suggest that stretch-activated ion channels and the PI3K/Akt pathway are critically involved in stretch-induced gene expression, although the link between stretch-activated ion channels and PI3K remains undetermined. Independence of the voltage-dependent Ca^{2+} channels, the mechanism of which is also observed in stretch-induced activation of heat-shock factor 1 (Chang et al., 2001), is a good contrast to their involvement in stretch-induced *BNP* expression. The PI3K/Akt pathway also contributes to stretch-induced activation of myocardial contractility (Petroff et al., 2001). Therefore, the Ca^{2+}/calmodulin pathway is involved in the hypertrophic responses, but distinct signaling pathways such as the PI3K/Akt pathways may be involved in other phenomena induced by mechanical stretch (Fig. 2).

7. Conclusion

Ca^{2+} plays a critical role in stretch-induced gene expression and ion channels may be one of "mechano-receptors" in cardiac myocytes. Further studies are necessary to clarify the role of voltage-dependent Ca^{2+} channels in mechanical stretch-induced gene expression.

8. Editor's note

Please see also related communications in this volume by Casadei and Sears (2003) and Calaghan et al. (2003).

Acknowledgements

This work was supported in part by grants from Japanese Ministry of Education, Science, Sports, and Culture, and Japan Health Sciences Foundation (to I.K.), and Japanese Heart Foundation (to H.A.). H.A. is a Research Resident for Research on Human Genome, Tissue Engineering Food Biotechnology of J.H.S.F.

References

Aiello, E.A., Villa, A.M., Cingolani, H.E., 2002. Autocrine stimulation of cardiac Na(+)-Ca(2+) exchanger currents by endogenous endothelin released by angiotensin II. Circ. Res. 90 (4), 374–376.

Allen, D.G., Kurihara, S., 1982. The effects of muscle length on intracellular calcium transients in mammalian cardiac muscle. J. Physiol. 327 (79), 79–94.

Calaghan, S.C., Belus, A., White, E., 2003. Do stretch-induced changes in intracellular calcium modify the electrical activity of cardiac muscle? Prog. Biophys. Mol. Biol. 82, 81–95.

Casadei, B., Sears, C.E., 2003. Nitric-oxide-mediated regulation of cardiac contractility and stretch responses. Prog. Biophys. Mol. Biol. 82, 67–80.

Chang, J., Wasser, J.S., Cornelussen, R.N., Knowlton, A.A., 2001. Activation of heat-shock factor by stretch-activated channels in rat hearts. Circulation 104 (2), 209–214.

Cingolani, H.E., Alvarez, B.V., Ennis, I.L., Camilion de Hurtado, M.C., 1998. Stretch-induced alkalinization of feline papillary muscle: an autocrine-paracrine system. Circ. Res. 83 (8), 775–80.

Dagnino, L., Lavigne, J.P., Nemer, M., 1992. Increased transcripts for B-type natriuretic peptide in spontaneously hypertensive rats. Quantitative polymerase chain reaction for atrial and brain natriuretic peptide transcripts. Hypertension 20 (5), 690–700.

Frey, N., McKinsey, T.A., Olson, E.N., 2000. Decoding calcium signals involved in cardiac growth and function. Nat. Med. 6 (11), 1221–1227.

Gruver, C.L., DeMayo, F., Goldstein, M.A., Means, A.R., 1993. Targeted developmental overexpression of calmodulin induces proliferative and hypertrophic growth of cardiomyocytes in transgenic mice. Endocrinology 133 (1), 376–388.

Hanford, D.S., Thuerauf, D.J., Murray, S.F., Glembotski, C.C., 1994. Brain natriuretic peptide is induced by alpha 1-adrenergic agonists as a primary response gene in cultured rat cardiac myocytes. J. Biol. Chem. 269 (42), 26227–26233.

Hongo, K., White, E., Le, G.J., Orchard, C.H., 1996. Changes in $[Ca^{2+}]i$, $[Na^{+}]i$ and Ca^{2+} current in isolated rat ventricular myocytes following an increase in cell length. J. Physiol.

Hu, H., Sachs, F., 1997. Stretch-activated ion channels in the heart. J. Mol. Cell. Cardiol. 29 (6), 1511–1523.

Hunter, J.J., Chien, K.R., 1999. Signaling pathways for cardiac hypertrophy and failure. N. Engl. J. Med. 341 (17), 1276–1283.

Irons, C.E., Sei, C.A., Hidaka, H., Glembotski, C.C., 1992. Protein kinase C and calmodulin kinase are required for endothelin-stimulated atrial natriuretic factor secretion from primary atrial myocytes. J. Biol. Chem. 267 (8), 5211–5216.

Kim, C.H., Cho, Y.S., Chun, Y.S., Park, J.W., Kim, M.S., 2002. Early expression of myocardial HIF-1alpha in response to mechanical stresses: regulation by stretch-activated channels and the phosphatidylinositol 3-kinase signaling pathway. Circ. Res. 90 (2).

Kirby, M.S., Sagara, Y., Gaa, S., Inesi, G., Lederer, W.J., Rogers, T.B., 1992. Thapsigargin inhibits contraction and Ca^{2+} transient in cardiac cells by specific inhibition of the sarcoplasmic reticulum Ca^{2+} pump. J. Biol. Chem. 267 (18), 12545–12551.

Komuro, I., Yazaki, Y., 1993. Control of cardiac gene expression by mechanical stress. Annu. Rev. Physiol. 55, 55–75.

Komuro, I., Kaida, T., Shibazaki, Y., Kurabayashi, M., Katoh, Y., Hoh, E., Takaku, F., Yazaki, Y., 1990. Stretching cardiac myocytes stimulates protooncogene expression. J. Biol. Chem. 265 (7), 3595–3598.

Komuro, I., Katoh, Y., Hoh, E., Takaku, F., Yazaki, Y., 1991a. Mechanisms of cardiac hypertrophy and injury—possible role of protein kinase C activation. Jpn. Circ. J. 55 (11), 1149–1157.

Komuro, I., Katoh, Y., Kaida, T., Shibazaki, Y., Kurabayashi, M., Hoh, E., Takaku, F., Yazaki, Y., 1991b. Mechanical loading stimulates cell hypertrophy and specific gene expression in cultured rat cardiac myocytes possible role of protein kinase C activation. J. Biol. Chem. 266 (2), 1265–1268.

Komuro, I., Kudo, S., Yamazaki, T., Zou, Y., Shiojima, I., Yazaki, Y., 1996. Mechanical stretch activates the stress-activated protein kinases in cardiac myocytes. FASEB J. 10 (5), 631–636.

Li, J., Hampton, T., Morgan, J.P., Simons, M., 1997. Stretch-induced VEGF expression in the heart. J. Clin. Invest. 100 (1), 18–24.

Mann, D.L., Kent, R.L., Cooper, G., 1989. Load regulation of the properties of adult feline cardiocytes: growth induction by cellular deformation. Circ. Res. 64 (6), 1079–1090.

McDonough, P.M., Glembotski, C.C., 1992. Induction of atrial natriuretic factor and myosin light chain-2 gene expression in cultured ventricular myocytes by electrical stimulation of contraction. J. Biol. Chem. 267 (17), 11665–11668.

Meguro, T., Hong, C., Asai, K., Takagi, G., McKinsey, T.A., Olson, E.N., Vatner, S.F., 1999. Cyclosporine attenuates pressure-overload hypertrophy in mice while enhancing susceptibility to decompensation and heart failure. Circ. Res. 84 (6), 735–740.

Molkentin, J.D., Lu, J.R., Antos, C.L., Markham, B., Richardson, J., Robbins, J., Grant, S.R., Olson, E.N., 1998. A calcineurin-dependent transcriptional pathway for cardiac hypertrophy. Cell 93 (2), 215–228.

Muth, J.N., Yamaguchi, H., Mikala, G., Grupp, I.L., Lewis, W., Cheng, H., Song, L.S., Lakatta, E.G., Varadi, G., Schwartz, A., 1999. Cardiac-specific overexpression of the alpha(1) subunit of the L-type voltage-dependent Ca(2+) channel in transgenic mice loss of isoproterenol-induced contraction. J. Biol. Chem. 274 (31), 21503–21506.

Muth, J.N., Bodi, I., Lewis, W., Varadi, G., Schwartz, A., 2001. A Ca(2+)-dependent transgenic model of cardiac hypertrophy: a role for protein kinase calpha. Circulation 103 (1), 140–147.

Ohmori, H., 1985. Mechano-electrical transduction currents in isolated vestibular hair cells of the chick. J. Physiol. 359, 189–217.

Pan, J., Fukuda, K., Saito, M., Matsuzaki, J., Kodama, H., Sano, M., Takahashi, T., Kato, T., Ogawa, S., 1999. Mechanical stretch activates the JAK/STAT pathway in rat cardiomyocytes. Circ. Res. 84 (10), 1127–1136.

Passier, R., Zeng, H., Frey, N., Naya, F.J., Nicol, R.L., McKinsey, T.A., Overbeek, P., Richardson, J.A., Grant, S.R., Olson, E.N., 2000. CaM kinase signaling induces cardiac hypertrophy and activates the MEF2 transcription factor in vivo. J. Clin. Invest. 105 (10), 1395–1406.

Perez, N.G., de, H.M., Cingolani, H.E., 2001. Reverse mode of the Na^{+}–Ca^{2+} exchange after myocardial stretch: underlying mechanism of the slow force response. Circ. Res. 88 (4), 376–382.

Petroff, M.G., Kim, S.H., Pepe, S., Dessy, C., Marban, E., Balligand, J.L., Sollott, S.J., 2001. Endogenous nitric oxide mechanisms mediate the stretch dependence of Ca^{2+} release in cardiomyocytes. Nat. Cell. Biol. 3 (10), 867–873.

Ramirez, M.T., Zhao, X.L., Schulman, H., Brown, J.H., 1997. The nuclear deltaB isoform of Ca^{2+}/calmodulin-dependent protein kinase II regulates atrial natriuretic factor gene expression in ventricular myocytes. J. Biol. Chem. 272 (49), 31203–31208.

Ruknudin, A., Sachs, F., Bustamante, J.O., 1993. Stretch-activated ion channels in tissue-cultured chick heart. Am. J. Physiol. 264 (3 Pt 2), H960–972.

Ruwhof, C., van Wamel, J.T., Noordzij, L.A., Aydin, S., Harper, J.C., van der Laarse, A., 2001. Mechanical stress stimulates phospholipase C activity and intracellular calcium ion levels in neonatal rat cardiomyocytes. Cell Calcium 29 (2), 73–83.

Sadoshima, J., Izumo, S., 1997. The cellular and molecular response of cardiac myocytes to mechanical stress. Annu. Rev. Physiol. 59 (551), 551–571.

Sadoshima, J., Takahashi, T., Jahn, L., Izumo, S., 1992. Roles of mechano-sensitive ion channels, cytoskeleton, and contractile activity in stretch-induced immediate-early gene expression and hypertrophy of cardiac myocytes. Proc. Natl. Acad. Sci. USA 89 (20), 9905–9909.

Sei, C.A., Irons, C.E., Sprenkle, A.B., McDonough, P.M., Brown, J.H., Glembotski, C.C., 1991. The alpha-adrenergic stimulation of atrial natriuretic factor expression in cardiac myocytes requires calcium influx, protein kinase C, and calmodulin-regulated pathways. J. Biol. Chem. 266 (24), 15910–15916.

Shimoyama, M., Hayashi, D., Takimoto, E., Zou, Y., Oka, T., Uozumi, H., Kudoh, S., Shibasaki, F., Yazaki, Y., Nagai, R., Komuro, I., 1999. Calcineurin plays a critical role in pressure overload-induced cardiac hypertrophy. Circulation 100 (24), 2449–2454.

Shimoyama, M., Hayashi, D., Zou, Y., Takimoto, E., Mizukami, M., Monzen, K., Kudoh, S., Hiroi, Y., Yazaki, Y., Nagai, R., Komuro, I., 2000. Calcineurin inhibitor attenuates the development and induces the regression of cardiac hypertrophy in rats with salt-sensitive hypertension. Circulation 102 (16), 1996–2004.

Sigurdson, W., Ruknudin, A., Sachs, F., 1992. Calcium imaging of mechanically induced fluxes in tissue-cultured chick heart: role of stretch-activated ion channels. Am. J. Physiol. 262 (4 Pt 2), H1110–1115.

Sussman, M.A., Lim, H.W., Gude, N., Taigen, T., Olson, E.N., Robbins, J., Colbert, M.C., Gualberto, A., Wieczorek, D.F., Molkentin, J.D., 1998. Prevention of cardiac hypertrophy in mice by calcineurin inhibition. Science 281 (5383), 1690–1693.

Thastrup, O., Cullen, P.J., Drobak, B.K., Hanley, M.R., Dawson, A.P., 1990. Thapsigargin, a tumor promoter, discharges intracellular Ca^{2+} stores by specific inhibition of the endoplasmic reticulum Ca2(+)-ATPase. Proc. Natl. Acad. Sci. USA 87 (7), 2466–2470.

Yamazaki, T., Tobe, K., Hoh, E., Maemura, K., Kaida, T., Komuro, I., Tamemoto, H., Kadowaki, T., Nagai, R., Yazaki, Y., 1993. Mechanical loading activates mitogen-activated protein kinase and S6 peptide kinase in cultured rat cardiac myocytes. J. Biol. Chem. 268 (16), 12069–12076.

Yamazaki, T., Komuro, I., Kudoh, S., Zou, Y., Shiojima, I., Mizuno, T., Takano, H., Hiroi, Y., Ueki, K., Tobe, K., 1995. Mechanical stress activates protein kinase cascade of phosphorylation in neonatal rat cardiac myocytes. J. Clin. Invest. 96 (1), 438–446.

Yamazaki, T., Komuro, I., Kudoh, S., Zou, Y., Nagai, R., Aikawa, R., Uozumi, H., Yazaki, Y., 1998. Role of ion channels and exchangers in mechanical stretch-induced cardiomyocyte hypertrophy. Circ. Res. 82 (4), 430–437.

Yang, X.C., Sachs, F., 1989. Block of stretch-activated ion channels in Xenopus oocytes by gadolinium and calcium ions. Science 243 (4894 Pt 1), 1068–1071.

Zhu, W., Zou, Y., Shiojima, I., Kudoh, S., Aikawa, R., Hayashi, D., Mizukami, M., Toko, H., Shibasaki, F., Yazaki, Y., Nagai, R., Komuro, I., 2000. Ca^{2+}/calmodulin-dependent kinase II and calcineurin play critical roles in endothelin-1-induced cardiomyocyte hypertrophy. J. Biol. Chem. 275 (20), 15239–15245.

Zou, Y., Hiroi, Y., Uozumi, H., Takimoto, E., Toko, H., Zhu, W., Kudoh, S., Mizukami, M., Shimoyama, M., Shibasaki, F., Nagai, R., Yazaki, Y., Komuro, I., 2001a. Calcineurin plays a critical role in the development of pressure overload-induced cardiac hypertrophy. Circulation 104 (1), 97–101.

Zou, Y., Yao, A., Zhu, W., Kudoh, S., Hiroi, Y., Shimoyama, M., Uozumi, H., Kohmoto, O., Takahashi, T., Shibasaki, F., Nagai, R., Yazaki, Y., Komuro, I., 2001b. Isoproterenol activates extracellular signal-regulated protein kinases in cardiomyocytes through calcineurin. Circulation 104 (1), 102–108.

Zou, Y., Yamazaki, T., Nakagawa, K., Yamada, H., Iriguchi, N., Toko, H., Takano, H., Akazawa, H., Nagai, R., Komuro, I., 2002. Continuous blockade of L-type Ca^{2+} channels suppresses activation of calcineurin and development of cardiac hypertrophy in spontaneously hypertensive rats. Hypertension Res. 25 (1), 117–124.

Available online at www.sciencedirect.com
SCIENCE DIRECT®
Journal of Molecular and Cellular Cardiology 35 (2003) 227–229
Journal of Molecular and Cellular Cardiology
www.elsevier.com/locate/yjmcc

Editorial

Too much Csx/Nkx2-5 is as bad as too little?

Cardiac transcription factors rule over the intricate process of coordinated myocardial differentiation by regulating cardiac-specific gene expression [1]. *Csx/Nkx2-5* is a member of NK homeobox gene family that is conserved in evolution and acts as a DNA-binding transcriptional activator [2–4]. Extensive investigation for the last decade has established the notion that Csx/Nkx2-5 is essential in normal cardiac development. Although considerable data have elucidated the roles of Csx/Nkx2-5 in cardiogenesis, little is known about functional significance of Csx/Nkx2-5 in the adult heart. On pages 243–256 of this issue of the *Journal of Molecular and Cellular Cardiology*, Kasahara et al. [5] demonstrated the unexpected role of Csx/Nkx2-5 in terminally differentiated cardiomyocytes by overexpressing wild-type or mutated Csx/Nkx2-5 protein both in murine heart and cultured cardiomyocytes.

Targeted disruption of *Csx/Nkx2-5* resulted in embryonic lethality due to the arrested looping morphogenesis of the heart tube [6,7]. In the heart of *Csx/Nkx2-5*-deficient embryos, expression of several cardiac genes was down-regulated including *ventricular isoform of myosin light chain 2*, *atrial natriuretic peptide* (*ANP*), *brain natriuretic peptide*, *cardiac ankyrin-repeat protein* (*CARP*), *MEF2C*, *eHAND/HAND1*, *N-myc*, *Iroquois homeobox gene 4*, and *HOP* [6–12], indicating the crucial role of Csx/Nkx2-5 in transcriptional regulation of a repertoire of cardiac-specific genes. Furthermore, many reports have been accumulated with regard to the molecular framework of transcriptional regulation by Csx/Nkx2-5. More cardiac genes are identified as direct downstream targets, such as *ANP* [13,14], *cardiac α-actin* [15], *A1 adenosine receptor* [16], *calreticulin* [17], *cardiac sodium-calcium exchanger 1 gene* [18], and *connexin 40* [10].

Csx/Nkx2-5 has attracted more attention since mutations in human *Csx/Nkx2-5* were reported to be responsible for a spectrum of congenital cardiac malformations associated with progressive atrioventricular conduction disturbance [19,20]. The promoter of *connexin 40* gene as well as that of *ANP* [21] is directly transactivated by Csx/Nkx2-5 in combination with T-box transcription factor, Tbx-5 [10]. Connexin 40 is a major constituent protein of gap junctions in the specialized conduction systems, and loss of *connexin 40* in mice enhances predisposition to cardiac conduction abnormalities [22,23]. Therefore, transcriptional regulation of gap junction proteins by Csx/Nkx2-5 is supposed to be relevant in maintaining the appropriate propagation of electrical activities in the heart.

Kasahara et al. [5] generated three types of transgenic mice, which overexpressed wild-type (TG-wild), a mutant lacking the C-terminus (TG-ΔC), or a DNA-nonbinding mutant with a missense mutation in the homeodomain (TG-I183P) under the control of the *α-myosin heavy chain* promoter to investigate the role of Csx/Nkx2-5 in the postnatal heart. To our surprise, all the transgenics, including TG-wild, displayed heart failure with conduction abnormalities. Furthermore, overexpression of *Csx/Nkx2-5* in cultured postnatal cardiomyocytes induced down-regulation of its potential downstream targets, such as *connexins*, *ANP* and *CARP*. From these findings, the authors came to the conclusion that transcriptional regulation of the individual target genes by Csx/Nkx2-5 diverges according to the developmental stages.

A number of works on molecular analysis of transcriptional regulation by Csx/Nkx2-5 were largely based on the experiments using the *Csx/Nkx2-5* mutant embryos or the data obtained by transient transfection assays using heterologous cell lines. Differential transcriptional regulation is implicated in cardiomyocytes with different spatial and temporal origins. Tbx-2 functions as a transcriptional repressor for *ANP* gene expression by displacing Tbx-5 and forming a complex with Csx/Nkx2-5 in the region of atrioventricular canal, inner curvature, outflow tract and inflow tract, where *Tbx-2* is expressed and *ANP* expression is exclusively absent [24]. Transcriptional activity of Csx/Nkx2-5 could be modulated positively and negatively by its respective endogenous-binding partner in a cell-type-specific manner. Identification of putative-binding partners of Csx/Nkx2-5 that determine its transcriptional mode in postnatal cardiomyocytes will be of great help to understand the intricate molecular mechanisms, where transcriptional activities switch from "promotive" to "repressive".

Another highly suggestive finding in this article is that, in neonatal cultured cardiomyocytes, adenoviral infection of wild-type *Csx/Nkx2-5* actually transactivated the *ANP* promoter, although endogenous mRNA of *ANP* was conversely down-regulated. As the authors mentioned in the text, it is possible that the promoter of *ANP* used in the reporter assays does not fully cover the regions where the *cis*-elements essential for practical transcriptional regulation in the biological context are located. The discrepancy may come from the intrinsic flaws of transient transfection assays, where the reporter plasmids are transactivated episomally. It would be

DOI: 10.1016/S0022-2828(03)00008-7

necessary to reconstitute comprehensively the molecular framework of transcriptional regulation by Csx/Nkx2-5 in postnatal cardiomyocytes. Serial analysis of the regulatory regions of each target gene using transgenic or knock-in reporter mice will provide mechanistic insights into the issue whether Csx/Nkx2-5 transactivates or repress the individual genes in the *in vivo* context.

We generated transgenic mice overexpressing human *Csx/Nkx2-5* under the control of cytomegalovirus enhancer/chicken β-*actin* promoter (WT-CSX TG) and reported that they appeared normal and did not show significant differences in cardiac performance evaluated by transthoracic echocardiography [25]. Expression levels of cardiac genes, such as *ANP*, *brain natriuretic peptide*, *CARP* and *ventricular isoform of myosin light chain 2* were up-regulated in adult hearts of WT-CSX TG mice. Electron microscopic analysis revealed that a number of secretory granules, which might contain ANP, were present in the ventricles of transgenics. Furthermore, we generated transgenic mice overexpressing dominant-negative mutant of CSX/NKX2-5, in which a highly conserved leucine in the homeodomain was substituted to a proline, under the control of *α-myosin heavy chain* promoter (DN-CSX TG) [26]. In DN-CSX TG mice, cardiac function was impaired, and degenerative changes of cardiomyocytes including loss of myofilaments and increased number of mitochondria were observed by electron microscopic analysis. DN-CSX TG mice showed severer cardiac dysfunction and larger number of apoptotic myocardial cells by injection of doxorubicin than wild types. On the contrary, doxorubicin-induced myocardial damages were mild in WT-CSX TG. These results indicate the essential role of CSX/NKX2-5 in protecting the cardiomyocytes from cytotoxic stress in the adulthood. In a feline pulmonary artery banding model, pressure overload induced right ventricular hypertrophy with increased expression levels of *Csx/Nkx2-5* and its downstream target genes, *ANP* and *cardiac α-actin* [27]. In this model, *Csx/Nkx2-5* transcript levels were increased significantly at 2 days after banding, and declined toward baseline levels after 2 weeks. Expression levels of *ANP* and *cardiac α-actin* changed in parallel with those of *Csx/Nkx2-5*, suggesting correlation of *Csx/Nkx2-5* expression with *ANP* and *cardiac α-actin* expression in adult heart.

How should these apparently contradictory phenotypes be interpreted? As Kasahara et al. speculated in the article, the functional gaps of human CSX/NKX2-5 vs. mouse Csx/Nkx2-5 might be the possible cause of the phenotypical differences. However, on the basis of the equivalent data obtained in the *in vitro* experiments, it is likely that Csx/Nkx2-5 proteins in both species should have the fundamental properties in common. Another possibility is that the phenotypes are dependent on the expression level of Csx/Nkx2-5 proteins. We previously reported that overexpression of a *Csx/Nkx2-5* mutant, with truncation of the C-terminus, induced apoptosis in cultured rat neonatal cardiomyocytes, although this mutant showed enhanced transactivation of the *ANP* promoter [28]. We examined at least two lines of WT-CSX TG and DN-CSX TG and found that there were good correlations between phenotypes and expression levels of the transgenes. We have not observed any mice with cardiac dysfunction, although they abundantly expressed wild type of Csx/Nkx2-5 protein. However, in the article by Kasahara et al., only one line in each type of transgenics was analyzed due to unsuccessful inheritance or scarce expression of the transgenes. Analysis of transgenic mice of different lines with divergent expression levels of wild-type Csx/Nkx2-5 would be informative to elucidate the postnatal function of Csx/Nkx2-5 in the heart.

The authors recently reported that transgenic mice overexpressing I183P mutant of *Csx/Nkx2-5* in the embryonic heart under the control of β-*myosin heavy chain* promoter were born normal, but exhibited cardiac conduction defect after birth with reduced expression levels of *connexin 43*, encoding a major component of gap junctions in working myocardium, as well as *connexin 40* [29]. The similar phenotypes of the previous transgenics and TG-I183P are accountable because expression of I183P mutant protein persisted after birth. However, our and their groups reported that Csx/Nkx2-5 mutants with missense mutations in the homeodomain, including I183P, operate as a dominant-negative transcriptional repressor *in vitro* [28,30]. If endogenous Csx/Nkx2-5 is a transcriptional repressor in the adult heart as demonstrated by the authors, this dominant-negative mutant is supposed to function as a transactivator! The authors noted that endogenous *Csx/Nkx2-5* expression was up-regulated in these transgenics and proposed that this mutant may operate as a hypomorphic gain-of-function mutant. Biochemical analysis is necessary to elucidate how I183P mutant modulate the function of Csx/Nkx2-5 in the adult cardiomyocytes.

Csx/Nkx2-5 may be lost in deep contemplation. "To be a transcriptional activator or a repressor? To be cardioprotective or cardiotoxic?" Further investigation will unravel the tangled web of unsolved questions with regard to transcriptional regulation by Csx/Nkx2-5 in the terminally differentiated cardiomyocytes.

References

[1] Bruneau BG. Transcriptional regulation of vertebrate cardiac morphogenesis. Circ Res 2002;90:509–19.

[2] Komuro I, Izumo S. Csx: a murine homeobox-containing gene specifically expressed in the developing heart. Proc Natl Acad Sci USA 1993;90:8145–9.

[3] Lints TJ, Parsons LM, Hartley L, Lyons I, Harvey RP. Nkx-2.5: a novel murine homeobox gene expressed in early heart progenitor cells and their myogenic descendants. Development 1993;119:419–31.

[4] Harvey RP. NK-2 homeobox genes and heart development. Dev Biol 1996;178:203–16.

[5] Kasahara H, Ueyama T, Wakimoto H, Liu MK, Maguire CT, Converso KL, et al. Nkx2.5 homeoprotein regulates expression of gap junction protein connexin 43 and sarcomere organization in postnatal cardiomyocytes. J Mol Cell Cardiol 2002;35:243–56.

[6] Lyons I, Parsons LM, Hartley L, Li R, Andrews JE, Robb L, et al. Myogenic and morphogenetic defects in the heart tubes of murine embryos lacking the homeobox gene Nkx2-5. Genes Dev 1995;9: 1654–66.

[7] Tanaka M, Chen Z, Bartunkova S, Yamasaki N, Izumo S. The cardiac homeobox gene *Csx/Nkx2.5* lies genetically upstream of multiple genes essential for heart development. Development 1999;126: 1269–80.

[8] Biben C, Harvey RP. Homeodomain factor Nkx2-5 controls left/right asymmetric expression of bHLH gene eHand during murine heart development. Genes Dev 1997;11:1357–69.

[9] Zou Y, Evans S, Chen J, Kuo HC, Harvey RP, Chien KR. CARP, a cardiac ankyrin repeat protein, is downstream in the Nkx2-5 homeobox gene pathway. Development 1997;124:793–804.

[10] Bruneau BG, Nemer G, Schmitt JP, Charron F, Robitaille L, Caron S, et al. A murine model of Holt-Oram syndrome defines roles of the T-box transcription factor Tbx5 in cardiogenesis and disease. Cell 2001;106:709–21.

[11] Chen F, Kook H, Milewski R, Gitler AD, Lu MM, Li J, et al. Hop is an unusual homeobox gene that modulates cardiac development. Cell 2002;110:713–23.

[12] Shin CH, Liu ZP, Passier R, Zhang CL, Wang DZ, Harris TM, Yamagishi H, et al. Modulation of cardiac growth and development by HOP, an unusual homeodomain protein. Cell 2002;110:725–35.

[13] Durocher D, Chen CY, Ardati A, Schwartz RJ, Nemer M. The atrial natriuretic factor promoter is a downstream target for Nkx-2.5 in the myocardium. Mol Cell Biol 1996;16:4648–55.

[14] Shiojima I, Komuro I, Oka T, Hiroi Y, Mizuno T, Takimoto E, et al. Context-dependent transcriptional cooperation mediated by cardiac transcription factors Csx/Nkx-2.5 and GATA-4. J Biol Chem 1999; 274:8231–9.

[15] Chen CY, Schwartz RJ. Recruitment of the tinman homolog Nkx-2.5 by serum response factor activates cardiac alpha-actin gene transcription. Mol Cell Biol 1996;16:6372–84.

[16] Rivkees SA, Chen M, Kulkarni J, Browne J, Zhao Z. Characterization of the murine A1 adenosine receptor promoter, potent regulation by GATA-4 and Nkx2.5. J Biol Chem 1999;274:14204–9.

[17] Guo L, Lynch J, Nakamura K, Fliegel L, Kasahara H, Izumo S, et al. COUP-TF1 antagonizes Nkx2.5-mediated activation of the calreticulin gene during cardiac development. J Biol Chem 2001;276: 2797–801.

[18] Muller JG, Thompson JT, Edmonson AM, Rackley MS, Kasahara H, Izumo S, et al. Differential regulation of the cardiac sodium calcium exchanger promoter in adult and neonatal cardiomyocytes by Nkx2.5 and serum response factor. J Mol Cell Cardiol 2002;34:807–21.

[19] Schott JJ, Benson DW, Basson CT, Pease W, Silberbach GM, Moak JP, et al. Congenital heart disease caused by mutations in the transcription factor NKX2-5. Science 1998;281:108–11.

[20] Benson DW, Silberbach GM, Kavanaugh MA, Cottrill C, Zhang Y, Riggs S, et al. Mutations in the cardiac transcription factor NKX2.5 affect diverse cardiac developmental pathways. J Clin Invest 1999; 104:1567–73.

[21] Hiroi Y, Kudoh S, Monzen K, Ikeda Y, Yazaki Y, Nagai R, et al. Tbx5 associates with Nkx2-5 and synergistically promotes cardiomyocyte differentiation. Nat Genet 2001;28:276–80.

[22] Simon AM, Goodenough DA, Paul DL. Mice lacking connexin40 have cardiac conduction abnormalities characteristic of atrioventricular block and bundle branch block. Curr Biol 1998;8:295–8.

[23] Kirchhoff S, Nelles E, Hagendorff A, Kruger O, Traub O, Willecke K. Reduced cardiac conduction velocity and predisposition to arrhythmias in connexin40-deficient mice. Curr Biol 1998;8:299–302.

[24] Habets PE, Moorman AF, Clout DE, Van RM, Lingbeek M, Van LM, et al. Cooperative action of Tbx2 and Nkx2.5 inhibits ANF expression in the atrioventricular canal: implications for cardiac chamber formation. Genes Dev 2002;16:1234–46.

[25] Takimoto E, Mizuno T, Terasaki F, Shimoyama M, Honda H, Shiojima I, et al. Up-regulation of natriuretic peptides in the ventricle of Csx/Nkx2-5 transgenic mice. Biochem Biophys Res Comm 2000; 270:1074–9.

[26] Toko H, Zhu W, Takimoto E, Shiojima I, Hiroi Y, Zou Y, et al. Csx/Nkx2-5 is required for homeostasis and survival of cardiac myocytes in the adult heart. J Biol Chem 2002;277:24735–43.

[27] Thompson JT, Rackley MS, O'Brien TX. Upregulation of the cardiac homeobox gene Nkx2-5 (CSX) in feline right ventricular pressure overload. Am J Physiol 1998;274:H1569–1573.

[28] Zhu W, Shiojima I, Hiroi Y, Zou Y, Akazawa H, Mizukami M, et al. Functional analyses of three Csx/Nkx-2.5 mutations that cause human congenital heart disease. J Biol Chem 2000;275:35291–6.

[29] Kasahara H, Wakimoto H, Liu M, Maguire CT, Converso KL, Shioi T, et al. Progressive atrioventricular conduction defects and heart failure in mice expressing a mutant Csx/Nkx2.5 homeoprotein. J Clin Invest 2001;108:189–201.

[30] Kasahara H, Lee B, Schott JJ, Benson DW, Seidman JG, Seidman CE, et al. Loss of function and inhibitory effects of human CSX/NKX2.5 homeoprotein mutations associated with congenital heart disease. J Clin Invest 2000;106:299–308.

Hiroshi Akazawa
Issei Komuro *
Department of Cardiovascular Science and Medicine, Chiba University Graduate School of Medicine
1-8-1 Inohana, Chuo-ku, Chiba 260-8670, Japan
E-mail address: komuro-tky@umin.ac.jp

Received 30 December 2002; accepted 31 December 2002

* Corresponding author.

Am J Physiol Regul Integr Comp Physiol 285: R581–R593, 2003.
First published May 15, 2003; 10.1152/ajpregu.00671.2002.

Attenuated defense response and low basal blood pressure in orexin knockout mice

Yuji Kayaba,[1,2] Akira Nakamura,[1] Yoshitoshi Kasuya,[3] Takashi Ohuchi,[4,5] Masashi Yanagisawa,[4,5] Issei Komuro,[2] Yasuichiro Fukuda,[1] and Tomoyuki Kuwaki[1,6]

Departments of [1]Autonomic Physiology, [2]Cardiovascular Science and Medicine, [3]Biochemistry and Molecular Pharmacology, and [6]Molecular and Integrative Physiology, Chiba University Graduate School of Medicine, Chiba-city, Chiba 260–8670; [4]ERATO, Japan Science and Technology, Tokyo 135–0064, Japan; and [5]Howard Hughes Medical Institute, Department of Molecular Genetics, University of Texas Southwestern Medical Center, Dallas, Texas 75235-9050

Submitted 31 October 2002; accepted in final form 14 May 2003

Kayaba, Yuji, Akira Nakamura, Yoshitoshi Kasuya, Takashi Ohuchi, Masashi Yanagisawa, Issei Komuro, Yasuichiro Fukuda, and Tomoyuki Kuwaki. Attenuated defense response and low basal blood pressure in orexin knockout mice. *Am J Physiol Regul Integr Comp Physiol* 285: R581–R593, 2003. First published May 15, 2003; 10.1152/ajpregu.00671.2002.—The perifornical area of the hypothalamus has been known as the center for the defense response, or "fight or flight" response, which is characterized by a concomitant rise in arterial blood pressure (AP), heart rate (HR), and respiratory frequency (Rf). We examined whether orexin, a recently identified hypothalamic neuropeptide, contributes to the defense response and basal cardiovascular regulation using orexin knockout mice. Microinjection of a GABA-A receptor antagonist, bicuculline methiodide (0.1–1 mM in 20 nl), to the perifornical area in urethane-anesthetized wild-type mice elicited dose-dependent increases in AP, HR, and Rf. Although similar changes were observed in orexin knockout mice, intensities were smaller and duration was shorter than those in wild-type mice. Moreover, in an awake and freely moving condition, telemeter-indwelling orexin knockout mice showed diminished cardiovascular and behavioral responses to emotional stress in the resident-intruder test. We also found that basal AP in orexin knockout mice was significantly lower in both anesthetized (117 ± 8 mmHg in wild type and 92 ± 3 in knockout) and conscious (125 ± 6 mmHg in wild type and 109 ± 2 in knockout) conditions. α-Adrenergic blockade with prazosin or ganglion blockade with hexamethonium canceled the difference in basal AP. HR and cardiac contractile parameters by echocardiography did not differ between the two strains of mice. These results indicate lower sympathetic vasoconstrictor tone in knockout mice. The present study suggests that orexin-containing neurons in the perifornical area play a role as one of the efferent pathways of defense response and also operate as a regulator of AP at basal condition by activating sympathetic outflow.

hypothalamus; stress; respiration; sympathetic nervous system; circadian rhythm

OREXIN A and B, also known as hypocretin 1 and 2, are recently identified neuropeptides that consist of 33 and 28 amino acids, respectively (10, 46). They are proteolytically derived from the same precursor peptide (prepro-orexin) and exert a variety of functions by acting on orexin receptor type 1 and/or type 2. Orexin-containing neuron cell bodies are located exclusively in the lateral and dorsal hypothalamic areas and their axons diffusely innervate almost the entire central nervous system (6, 9, 10, 38, 39, 44, 46). This anatomic feature establishes the bases that orexin contributes to multiple physiological functions, including feeding behavior (46), energy homeostasis (46, 54), sleep-wake cycle (5), and regulation of the autonomic and neuroendocrine systems (9, 22, 44, 54).

Several laboratories have proposed a possible contribution of orexin in cardiovascular regulation by observing the effects of exogenously administered orexins. Orexins on intracerebroventricular injection increased arterial blood pressure (AP), heart rate (HR) (47), renal sympathetic nerve activity, and plasma catecholamines (50) in conscious, unrestrained rats. Intrathecal administration of orexins increased AP and HR (3). Microinjection of orexin A to the rostral ventrolateral medulla (RVLM) increased AP and HR in anesthetized rats (7) and awake rats (36). However, there is no report to date on whether the same is true for intrinsic orexin.

On the other hand, the perifornical area of the hypothalamus or dorsomedial hypothalamus, a region of the brain with the highest density of orexin-containing neurons (9, 10, 44, 46), has been known as the center for defense response and is sometimes called the defense area (29). Defense response, which is also known as "fight-or-flight" response, is characterized by a coordinated rise in AP, HR, respiratory frequency (Rf), and resistance in most vascular beds along with a fall in resistances in airway and blood vessels in the skeletal muscles when an animal encounters stressors. A pioneer work by Hess (23) showed that electrical stimulation of the posterior hypothalamus in cats elicited behavioral rage, along with the specific autonomic responses, that was termed the "defense response." Although some reports using chemical stimulation with

Address for reprint requests and other correspondence: T. Kuwaki, Dept. of Molecular and Integrative Physiology, Chiba Univ. Graduate School of Medicine, 1–8-1 Inohana, Chuo-ku, Chiba 260–8670, Japan (E-mail: kuwaki@faculty.chiba-u.jp).

The costs of publication of this article were defrayed in part by the payment of page charges. The article must therefore be hereby marked "*advertisement*" in accordance with 18 U.S.C. Section 1734 solely to indicate this fact.

excitatory amino acids (e.g., glutamate) had shown no effect or even a depressor effect (19, 25), later it was shown that negative results might have been caused by the stimulation of specific subregions in the posterior hypothalamus and/or dosage of drugs (14). Actually, the perifornical area was the most reliable region to elicit the cardiovascular defense response (29), and an overdose of excitatory amino acids sometimes inhibited neuronal activity, an effect known as excitation block phenomenon (34). Disinhibition with a GABA-A receptor antagonist, bicuculline methiodide, of the perifornical area reliably and dose dependently induced the defense response (13). Moreover, injection of a GABA agonist to the defense area inhibited the stress-induced rise in AP and HR (35).

There is only limited information about neurotransmitter(s) that subserve efferent pathways of the defense responses. Namely, glutamate was proposed to mediate at least the cardiovascular component of the defense response (52). However, there is no report on the molecular basis of the defense response underlying its multifaceted nature such as concomitant and coordinated changes in cardiovascular, respiratory, and behavioral parameters. We hypothesized that intrinsic orexin, synthesized in the perifornical area, may participate in the efferent pathway of the defense response and thought that knockout mice may be useful to test the hypothesis.

Prepro-orexin knockout mice, which completely lack both orexin A and orexin B, have been recently established (5). They exhibited a phenotype strikingly similar to human narcolepsy patients, such as behavioral arrest resembling cataplectic attack, sleep-onset rapid eye movement sleep, and diminished awake time in the dark period. This murine model and the canine model of narcolepsy that has mutation in the gene for orexin receptor type-2 (33) suggested the importance of orexin-orexin receptor type-2 interaction in the pathogenesis of narcolepsy. In fact, human narcolepsy seems to be an autoimmune disease, resulting in loss of orexin-containing neurons in the hypothalamus (53). On the other hand, there are only a few reports examining autonomic regulation in human narcolepsy (see DISCUSSION). Cardiovascular and autonomic phenotypes in orexin knockout mice have not been examined.

The aim of this study was to test our hypothesis by *1*) identifying hypothalamic subregion(s) in mice suitable to elicit the defense response and by *2*) comparing the effect of hypothalamic stimulation between orexin null mutated knockout mice and wild-type mice. Possible involvement of orexin in the defense response was further clarified by *3*) telemetric measurement of AP and HR during socioemotional stress of the resident-intruder test. In the course of the experiments, we found lower basal AP in orexin knockout mice. Therefore, an additional aim of this study was to examine possible involvement of intrinsic orexin in basal cardiovascular regulation by *4*) comparing AP and HR between mutant and wild-type mice in unanesthetized freely moving condition with or without pharmacological perturbations.

MATERIALS AND METHODS

Animals. Prepro-orexin mutated mice of genetic background of a mixture of 129/Sv and C57BL/6 were generated as reported previously (5). They were maintained in heterozygotes and crossed to obtain null mutants and wild-type littermates. Genotype of orexin knockout mice was identified by PCR on DNA extracted form a tail biopsy in a similar manner as had been reported except for primer sequences. We used a 5′ primer, GAC CTA TCA GGA CAT AGC GTT GGC and a 3′ primer, TCA CCC CCT TGG GAT AGC CCT TCC for the mutant allele and a 5′ primer, GAC GAC GGC CTC AGA CTT CTT GGG with the same 3′ primer to identify the wild-type allele. Mice used in this study were 18- to 40-wk-old male orexin null mutated mice and wild-type mice. Heterozygotes were not used. All mice were housed in plastic cages in a room maintained at 23–25°C with lights on at 7:00 AM and off at 7:00 PM. Mice had food and water available ad libitum. All animal procedures conformed to the "Guiding Principles for the Care and Use of Animals in the Field of Physiological Sciences" recommended by the Physiological Society of Japan.

Measurement of cardiorespiratory parameters and electroencephalogram in anesthetized mice. Mice were anesthetized with intraperitoneal injection of urethane (1.1 g/kg); supplementary doses of 0.1–0.5 g/kg were given when required to maintain a level of anesthesia (average total dose including all additional doses was 1.22 ± 0.05 g/kg, n = 20). We found this dose was adequate in both orexin knockout mice and wild-type mice as judged by baseline stability of AP, HR, respiration, and electroencephalography (EEG) throughout the experiment. Cardiorespiratory parameters were recorded as described in our previous reports (31, 42). In brief, AP was measured by a pressure sensor catheter (SPR-671 microtip pressure catheter for mouse/rat, Millar, Houston, TX) placed in the abdominal aorta through an incision of the right femoral artery. Mean AP (MAP) was calculated by damping (0.2 Hz low pass) the phasic AP signal. HR was recorded using an HR counter (AT-601G, Nihon Kohden, Tokyo, Japan) triggered by the AP pulse. A tracheal cannula (polyethylene tube, OD = 1.20 mm) was inserted through a midline incision. Respiratory flow signal was obtained through a Lilley type pneumotachograph (TV-241T and TP-602T, Nihon Kohden) connected to the tracheal tubing. Rf was counted by a pulse counter (ET-612J, Nihon Kohden). In *experiment 2* (see below), a pair of electrodes to record EEG was implanted through holes in the skull over the left and right frontal cortex. Cortical EEG arousal has been implicated as one of the functions of the perifornical lateral hypothalamus (11) and may be a part of defense response. EEG signals were amplified with band-pass filters of 0.25–100 Hz (AB-651J, Nihon Kohden). In *experiment 1*, we did not try to measure EEG because electrical stimulation in the brain makes serious noise in EEG.

In both *experiments 1* and *2*, the animal was placed in the prone position in a stereotaxic frame (ST-7, Narishige, Tokyo, Japan) so that bregma and lambda would be horizontal. A small hole was drilled on the skull for insertion of a metal electrode or a glass micropipette into the hypothalamus. After completion of surgery, at least 1 h was allowed to stabilize all the parameters. Throughout the experiment, rectal temperature was kept constant at 37.0 ± 1.0°C by a heating pad connected to a thermo controller (ATB-1100, Nihon Kohden).

Experiment 1: mapping of hypothalamic areas to induce defense response. We used 18- to 25-wk-old male wild-type mice (n = 10, body wt 32 ± 3 g). Electrical stimulations were

made with stainless steel electrodes. Explored brain regions were the perifornical area and surrounding hypothalamus (from 1.5 to 2.5 mm caudal to the bregma, from 0.3 to 1.5 mm lateral to the midline, and from 4.0 to 5.8 mm ventral to the bregma). An enamel-coated sharp stainless-steel electrode (0.1 mm of the tip exposed) was inserted into the targeted region, and the different lead was placed under the skin of the neck. The electrode was carried in a stereotaxic micromanipulator (SM-11, Narishige) and lowered along the track in steps of 0.3 mm. Three to seven tracks were completed in each animal, and each track was 0.5 mm apart from the other tracks. At each point, the brain was stimulated with a train of rectangular pulses of 0.5-ms duration at 100 Hz for 20 s. The stimulation currents were 0.3 mA with the negative electrode. Stimulations were separated by at least 5 min after all the parameters returned to baseline. We used electrical stimulation in *experiment 1* because repeated drug injection to such a tiny brain as in mice cannot be devoid of volume effect (34). However, electrical stimulation excites not only cell bodies but also fibers of passage. Because of such a disadvantage in electrical stimulation, we used the microinjection technique in *experiment 2* (see below) to stimulate only cell bodies but not fibers of passage.

Experiment 2: chemical stimulation of the perifornical area. Experiments were done in 18- to 25-wk-old male wild-type mice (n = 5, body wt 35 ± 1 g) and prepro-orexin knockout mice (n = 5, 36 ± 2 g). Microinjection of drugs was made with glass micropipettes (Drummond, 1–5 μl) shaped by a micropipette puller (PE-2, Narishige) and cut to fit the tip diameter of 20–30 μm. The pipettes were carried in a stereotaxic micromanipulator (SM-11, Narishige) and connected by silicon tubing to a pressure injector (IM-200J, Narishige). The micropipette was filled with a GABA-A receptor antagonist, bicuculline methiodide (0, 0.1, 0.3, 1.0 mM), dissolved in artificial cerebrospinal fluid (ACSF). The tip of the pipette was positioned in the perifornical area, where maximum response was observed in *experiment 1* (2.0 mm caudal to the bregma, 0.65 mm lateral to the midline, 5.0 mm ventral to the bregma, see also Fig. 1). While observing the fluid meniscus in the micropipette through a dissection microscope (OME, Olympus) equipped with an ocular micrometer, a volume of 20 nl was injected by adjusting pressure and time of injection. Bicuculline was administered sequentially from the lowest dose to the highest after recorded parameters returned to the baseline in each animal.

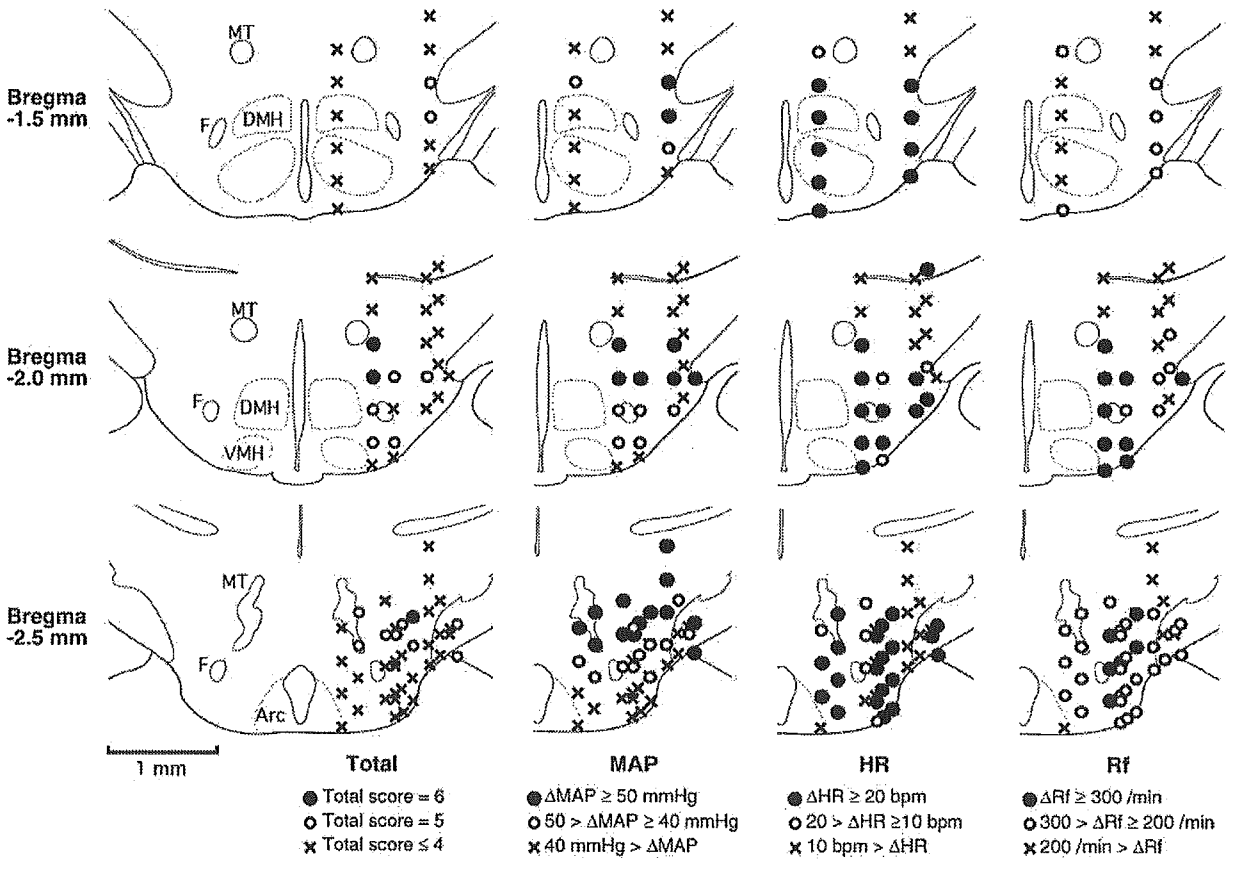

Fig. 1. Schematic coronal sections of the mouse hypothalamus from 1.5 to 2.5 mm caudal to the bregma showing effects of electrical stimulation on (*left* to *right*) consolidated defense response (Total), mean arterial blood pressure (MAP), heart rate (HR), and respiratory frequency (Rf). Data were obtained from 10 wild-type (WT) mice. Arc, arcuate hypothalamic nucleus; DM, dorsomedial hypothalamic nucleus; F, fornix; MT, mammillothalamic tract; VMH, ventromedial hypothalamic nucleus.

Experiment 3: measurement of cardiovascular parameters and activity by radiotelemetry. Experiments were done in 30- to 40-wk-old male wild-type mice (n = 6, body wt 46 ± 3 g) and prepro-orexin knockout mice (n = 6, 52 ± 2 g). A telemetry system (Data Sciences International) was used for measuring AP, HR, and locomotor activity. This system consisted of a radio-frequency transducer (TA11PA-C20) and a receiver (RLA1020). For implantation of the transducer, mice were anesthetized with 2–3% isoflurane and given an antibiotic (cephalosporin, 50 mg/kg sc). A midline incision was made on the neck, and the left common carotid artery was isolated. A small cut was made in the vessel wall, and the catheter-transducer was implanted in the thoracic aorta through the hole. The sensor was tunneled subcutaneously and fixed to the abdominal wall. Finally, the incision was closed with sutures. Care was taken to maintain body temperature during and after the surgery. Mice were returned to their home cages and housed individually during the recovery and recording period. All the mice were allowed at least 5 days of recovery from surgery until circadian rhythm was evident in both AP and HR (4).

After the recovery period, AP, HR, and activity were recorded for successive 2–3 days using Dataquest LabPRO software (Data Sciences) in unrestrained, freely moving, and unanesthetized conditions.

Two types of stressor were applied in the afternoon on the following day after the basal measurement was completed. The first one was a socioemotional stressor in the resident-intruder test (31). A group-housed, age-matched wild-type mouse (intruder) was placed in the cage for 5 min. When AP, HR, and activity returned to the baseline, a second trial of the resident-intruder test was performed, but the telemeter-indwelling animal served as the intruder this time. Cardiovascular and behavioral responses in the first and second trials in the resident-intruder test are called "resident response" and "intruder response," respectively, in this study. The second stressor was noxious stimuli. Vascular clamps of two strengths (60 and 125 g, Fine Science Tools, nos. 18055–01 and -04) were attached to the tail for 10 s.

Finally, on the following day in the light phase, urethane (1.1 g/kg) was intraperitoneally administered to see whether the difference in AP observed in *experiment 2* (see RESULTS) could be reproduced and to confirm that attenuation of defense response observed in *experiment 2* did not result from generally increased susceptibility of the knockout mice to anesthesia.

Experiment 4: measurement of cardiovascular parameters with indwelling catheter and pharmacological interventions. Experiments were done in 18- to 25-wk-old male wild-type mice (n = 21, body wt 33 ± 1 g) and prepro-orexin knockout mice (n = 14, 33 ± 1 g). For simultaneous AP measurement and intravascular drug delivery, we used an indwelling catheter to minimize surgical damage because telemetric AP measurement needs additional operation for this purpose. Under isoflurane anesthesia, polyethylene tubing was inserted into the femoral artery for both AP measurement and drug delivery as reported (41). On the following day during the light phase, AP and HR were measured continuously for 2 h under conscious and unrestrained conditions in a quiet environment after at least 1 h of acclimatization. Thereafter, the animals were divided into three groups. The first group was given intra-arterially a ganglion blocker, hexamethonium (20 mg/kg, n = 13 in wild-type mice and n = 6 in knockout mice), to examine possible contribution of the autonomic nervous system in the difference in basal AP between knockout and wild-type mice. The second group was given an angiotensin-converting enzyme inhibitor, captopril (30 mg/kg, n = 3 in both wild-type and knockout mice), to examine possible interaction of ANG II and orexin, since orexin has been shown to stimulate drinking behavior as potently as ANG II (30). The third group (n = 5 in both wild-type and knockout mice) was sequentially given two drugs: a vasopressin V1a receptor antagonist, [β-mercapto-β,β-cyclopentamethylenepropionyl[1], O-me-Tyr[2], Arg[8]]vasopressin (10 μg/kg), and an α-adrenergic blocker, prazosin (1 mg/kg). Effect of the V1 receptor antagonist was tested because orexin-containing neurons innervate neurons in the paraventricular nucleus containing vasopressin (51). Resulting AP and HR were calculated as the peak value within 1 h after the administration.

Experiment 5: measurement of echocardiography. Experiments were done in 14- to 18-wk-old male wild-type mice (n = 6) and prepro-orexin knockout mice (n = 6). Anesthetized (pentobarbital sodium, 50 mg/kg ip) animals were observed with a 2D-guided M-mode echocardiographic system equipped with a 12-MHz imaging transducer (Sonos 4500; Agilent Technologies, Osaka, Japan). Left ventricular (LV) diastolic diameter (LVDD) and LV systolic diameter (LVSD) were measured. LV end-diastolic volume (LVEDV) and LV end-systolic volume (LVESV) were calculated by the cubed method as $(LVDD)^3\pi/3$ and $(LVSD)^3\pi/3$, respectively. We also calculated percent fractional shortening [%FS = 100 × (LVDD − LVSD)/LVDD], stroke volume (SV = LVEDV − LVESV), and ejection fraction (%EF = 100 × SV/LVEDV). Three beats were averaged for each measurement.

Data analysis and statistical procedure. All the signals were fed into a personal computer (Macintosh, Apple Computer) after analog-to-digital conversion (model 1401, CED, UK or MacLab, AD Instrument, Australia) together with event signals.

In *experiment 1*, the baseline value was the mean value before stimulation for 20–30 s, and the peak value was calculated as a mean value for 5–10 s around the maximum response.

In *experiment 2*, data were averaged for every 1 min. The baseline value was the mean value during 5 min before injection of bicuculline. Recovery time was defined as the time from injection until MAP, HR, or Rf returned to the value 5% above the baseline, because spontaneous fluctuation of these parameters during control period was within ±5% range of the mean value. We also calculated the area under the curve (AUC) above the baseline value during periods of 10, 15, 20, and 30 min from the injection for 0, 0.1, 0.3, and 1.0 mM of bicuculline, respectively. The length of the periods was determined from the result of recovery time in wild-type mice (see Table 1). To estimate the cortical arousal level, we calculated the power spectra of EEG using fast Fourier transformation (FFT; length of sections 5 s, FFT number 512). Arousal level was determined as relative β-band (13–50 Hz) power to the total band powers. For relative β-band power, recovery was defined as the time point when the value returned to a value 20% above the baseline, since spontaneous fluctuation of this parameter during control period was within ±20% range of the mean value.

For circadian measurement in *experiment 3*, AP, HR, and activity counting were averaged for every 30 min. Values in each animal were analyzed by the cosinor method (40) to calculate midline estimating statistic of rhythm (MESOR) and amplitude. The mean light and dark phase values were also calculated. In the resident-intruder test, AP, HR, and activity counting were averaged for every 1 min. AUC was calculated for 5 min when resident and intruder were in the same cage. In the tail-clip test, resulting AP and HR were calculated as the peak value within 30 s after the start of

Table 1. *Duration of responses by bicuculline*

Parameter	Dose of Bicuculline, mM in 20 nl	Wild-Type Mice	Knockout Mice
Blood pressure	0.1	10.8 ± 2.6	2.6 ± 1.7*
	0.3	15.8 ± 2.9	5.0 ± 1.6*
	1	26.0 ± 2.7	14.0 ± 2.2*
Heart rate	0.1	12.4 ± 1.6	1.8 ± 1.1*
	0.3	22.8 ± 2.4	9.0 ± 2.8*
	1	31.8 ± 2.3	25.2 ± 5.5
Respiratory frequency	0.1	12.4 ± 1.6	1.6 ± 1.0*
	0.3	19.2 ± 2.8	9.4 ± 1.4*
	1	21.2 ± 2.6	19.6 ± 3.7
EEG β-band power	0.1	11.0 ± 1.0	2.2 ± 0.9*
	0.3	18.8 ± 2.2	8.6 ± 2.6*
	1	28.2 ± 4.7	11.0 ± 1.4*

Values are means ± SE of response duration in min. *$P < 0.05$ vs. wild-type mice (repeated-measure ANOVA followed by post hoc test of Student-Newman-Keuls).

clipping. In urethane treatment, pretreatment value was calculated as the mean during the 0.5 h immediately before injection. Posttreatment value was the average during the period from 1 to 6 h after injection, since *experiment 2* was usually completed within 6 h.

All data are expressed as means ± SE. Effects of microinjection of bicuculline on cardiovascular, respiratory, and arousal responses were assessed by ANOVA with repeated measures design. Post hoc comparisons of Student-Newman-Keuls procedure or unpaired *t*-test were used to compare between genotypes. A value of $P < 0.05$ was considered significant.

Histological verification of stimulation sites. At the end of the experiment, the injection site was marked by injecting 20 nl of a 2% Evans blue solution in *experiment 2*. In *experiment 1*, the same Evans blue solution was injected to the site where electrical stimulation was finally performed. The animal was deeply anesthetized with additional urethane and transcardially perfused with 20 ml of heparin-added saline followed by 20 ml of 4% formalin. The brains were removed and stored in the formalin solution for at least 2 days before sectioning. Coronal or sagittal sections of 50-μm thickness were cut serially with a micro slicer (DTK-1000, Dosaka EM, Kyoto, Japan), mounted on poly-L-lysine-coated slides, and stained with 1% neutral red or 0.5% cresyl violet. The locations of the injection sites were determined according to the atlas of Paxinos and Franklin (43).

RESULTS

Experiment 1: mapping of hypothalamic areas to induce defense response. To examine whether hypothalamic stimulation induces defense response in mice as in other experimental animals, the effect of electrical stimulation on cardiorespiratory parameters was systematically explored. Ninety-three histologically verified sites within the targeted area were examined in 10 mice. Average MAP, HR, and Rf before stimulation were 115 ± 4 mmHg, 570 ± 15 beats/min, and 194 ± 5/min, respectively. Electrical stimulation in most sites resulted in increases in MAP, HR, and Rf except for 11 sites to which stimulation resulted in decreases in HR. Response magnitude of each parameter was ranked into three levels and is shown in Fig. 1. Stimulation at caudal hypothalamic sites induced a pressor response. The most effective sites were located in the dorsolateral region in the caudal hypothalamus, where electrical stimulation resulted in an increase in MAP by >50 mmHg (Fig. 1). In regard to HR, effective sites were roughly overlapped with but extended more widely compared with the effective sites for MAP. Electrical stimulation at most of the explored sites in the caudal hypothalamus produced an increase in HR by >20 beats/min. An increase in Rf was elicited in the middle to lateral part of the caudal hypothalamus, in which responses in Rf were >300/min.

To map the most effective sites for eliciting defense response, in other words coordinated increases in MAP, HR, and Rf, the rank of response magnitude in each parameter was scored as 2, 1, or 0 points from the highest to the lowest in this order, and summation of scores was calculated for each stimulating site (Fig. 1, *left*). The total score was highest at three sites in the dorsal part of the perifornical area. The most effective sites were located at 0.65 mm lateral to the midline, 4.7–5.0 mm ventral to the bregma in the plane of 2.0 mm caudal to the bregma, and 1.0 mm lateral, 4.7 mm ventral in the plane of 2.5 mm caudal to the bregma.

These results clearly show that defense response can be elicited by electrical stimulation of dorsal hypothalamus, especially the dorsal part of the perifornical area in mice. From these results, we decided to stimulate a point 2.0 mm caudal to the bregma, 0.65 mm lateral to the midline, and 5.0 mm ventral to the bregma in the following experiment.

Experiment 2: chemical stimulation of the perifornical area in orexin knockout mice. To test our hypothesis that orexin may contribute to expression of the defense response, we compared the effects of chemical stimulation with bicuculline to the perifornix on cardiorespiratory and EEG parameters between orexin null mutated knockout mice and wild-type littermates. Before stimulation, the average values of MAP, HR, Rf, and relative β-power in five wild-type mice were 117 ± 8 mmHg, 558 ± 12 beats/min, 178 ± 7/min, and 14 ± 2%, respectively. In wild-type mice, microinjection of 0.1–1 mM of bicuculline to the perifornical area elicited dose-dependent increases in MAP, HR, Rf, and relative β-power (Fig. 2), but ACSF (vehicle) did not cause any significant changes. By 0.1, 0.3, and 1.0 mM of bicuculline, peak increases in MAP (11 ± 2%, 13 ± 1, and 28 ± 2%), HR (13 ± 3, 17 ± 2, and 19 ± 4%), Rf (54 ± 6, 103 ± 7, and 167 ± 15%), and relative β-power (111 ± 22, 122 ± 39, and 121 ± 17%) were all statistically significant. These changes began within 15 s from injection of bicuculline and returned to baseline within 10–30 min depending on the dosage (Table 1).

In orexin knockout mice, basal values of MAP, HR, Rf, and relative β-power were 92 ± 3 mmHg, 562 ± 22 beats/min, 218 ± 11/min, and 13 ± 3%, respectively. MAP was significantly ($P < 0.05$) lower and Rf was significantly higher than that in wild-type mice (Fig. 2). Basal HR and relative β-power were not significantly different between the genotypes. At a glance, microinjection of bicuculline to the perifornical area in the mutant mice appeared to result in similar cardio-

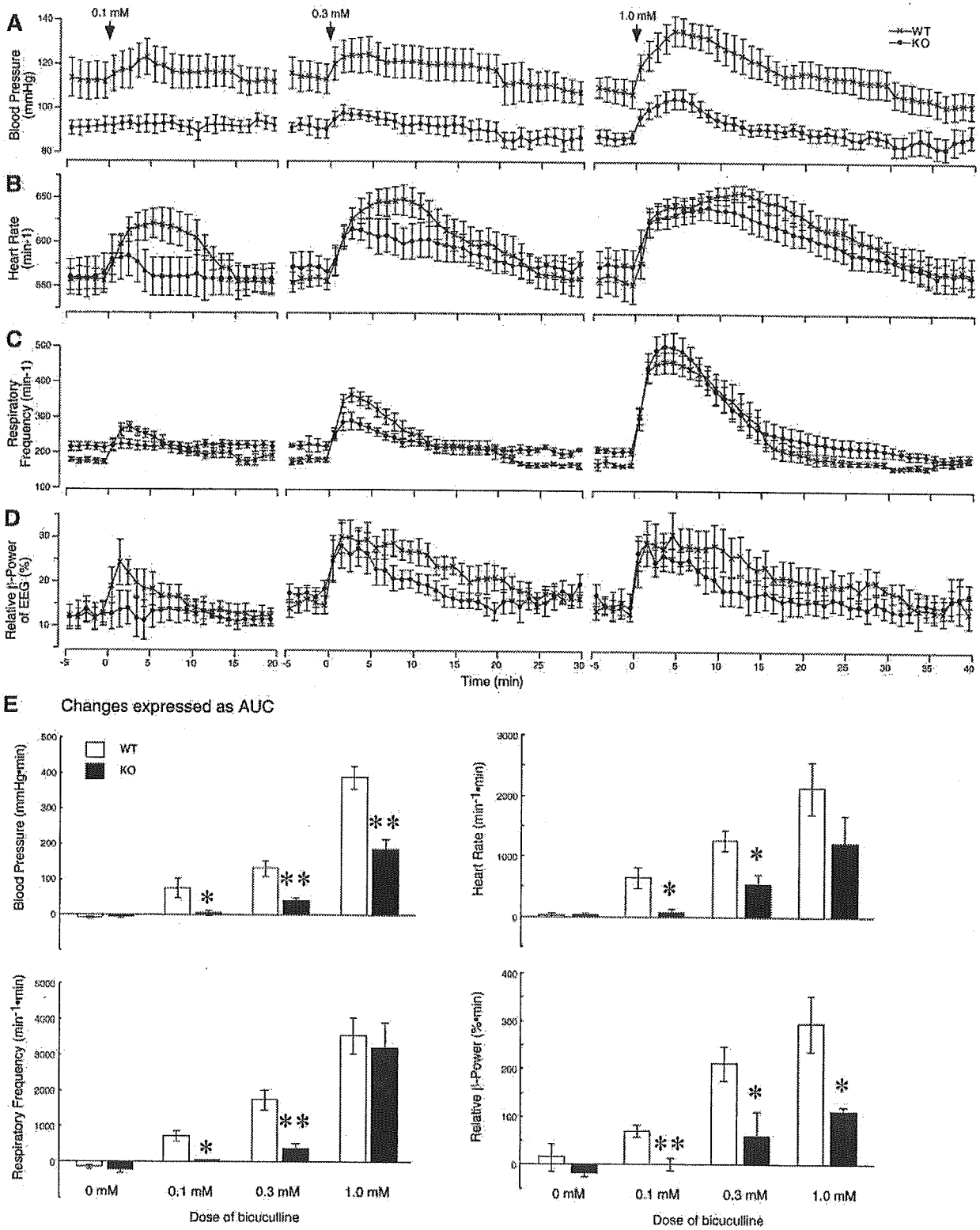
A
B
C
D
E
0.1 mM
0.3 mM
1.0 mM
WT
KO
Blood Pressure (mmHg)
Heart Rate (min-1)
Respiratory Frequency (min-1)
Relative β-Power of EEG (%)
Time (min)
Changes expressed as AUC
Blood Pressure (mmHg•min)
Heart Rate (min-1•min)
Respiratory Frequency (min-1•min)
Relative β-Power (%•min)
0 mM
0.1 mM
0.3 mM
1.0 mM
Dose of bicuculline

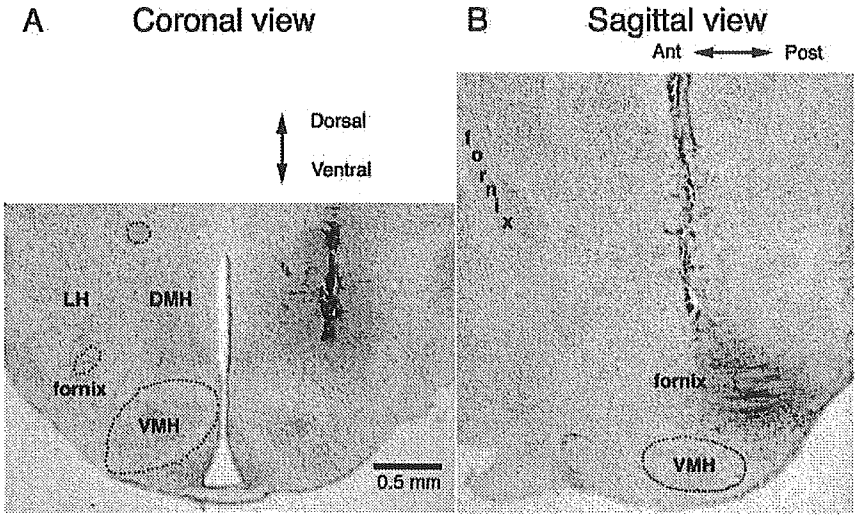

Fig. 3. Photomicrographs of coronal (*A*, at the level of 2 mm caudal to the bregma) and sagittal (*B*, at the level of 0.65 mm lateral to the midline) sections through the hypothalamus prepared after the experiment. Injection site of bicuculline was marked with Evans blue. Each section was stained with 1% neutral red. Ant, anterior; Post, posterior.

respiratory responses to those in wild-type mice (Fig. 2). In detailed analysis, however, there was a significant quantitative difference between knockout mice and wild-type mice. Whereas 0.1 mM of bicuculline was effective to elicit significant changes in MAP, HR, and Rf in wild-type mice, the same dose of bicuculline did not cause any significant changes in the knockout mice (Fig. 2, *A–D*, *left*), except for a small and shortlasting increase in HR. At the dose of 0.3 mM, cardiorespiratory responses in the knockout mice were shorter lasting than those in wild-type mice (Fig. 2, *A–D*, *middle*, and Table 1). At the dose of 1.0 mM, responses in AP and EEG were still shorter lasting although recovery time of HR and Rf responses was not statistically different from the wild-type mice (Fig. 2, *A–D*, *right*, and Table 1). Consequently, response magnitudes as calculated by AUC were significantly smaller in knockout mice for all the parameters (Fig. 2*E*) at least for 0.1 and 0.3 mM of bicuculline.

By histological examination, there was no difference in the dye distribution between wild-type mice and orexin knockout mice, and all the injections were successfully made in dorsal part of the perifornical area (Fig. 3).

Experiment 3: measurement of cardiovascular parameters and activity by radiotelemetry. Attenuation of defense response in orexin knockout mice was further confirmed by radiotelemetric measurement of behavioral and cardiovascular parameters in unanesthetized freely moving mice with a natural stressor (Fig. 4). At the baseline before stress, low AP and similar HR in orexin knockout mice were observed as was the case in anesthetized condition. When the test animal was confronted with an intruder, increases in AP, HR, and activity were significantly smaller in orexin knockout mice than in wild-type mice (Fig. 4*A*). The same was true when the test animal intruded into a resident's home cage (Fig. 4*B*). On the other hand, noxious stimuli of the tail pinch elicited similar increases in AP and HR in both genotypes, irrespective of stimulus intensity (Fig. 5).

We next examined circadian rhythm of AP, HR, and activity in the orexin knockout mice, because deficiency of orexin has been shown to induce disturbance in sleep-awake cycle and thus may induce abnormality in circadian rhythm of cardiovascular parameters. Activity during dark phase but not during light phase was significantly lower in orexin knockout mice and thus amplitude of 24-h fluctuation in activity was significantly lower in the mutant mice (Fig. 6, Table 2). Contrary to our expectation, however, circadian fluctuation of AP and HR was similar between knockout and wild-type mice except that AP in knockout mice was consistently lower during both dark phase and light phase. Although amplitude of AP in orexin knockout mice tended to be smaller, the difference did not reach statistical significance ($P = 0.34$).

To exclude the possibility that basal hypotension in orexin knockout mice in *experiment 2* was due to a difference in sensitivity to anesthetic, we next examined the effect of urethane administration on AP and HR in radiotelemeter-indwelling mice. As expected, urethane lowered AP in a similar manner in mutant (before urethane, 108 ± 3 mmHg and after, 83 ± 5 mmHg, −23.5 ± 3.5%) and wild-type mice (before urethane, 127 ± 6 mmHg and after, 102 ± 7 mmHg, −19.7 ± 3.6%). HR was not different between knockout

Fig. 2. Effects of microinjection of bicuculline methiodide to the perifornical area in urethane-anesthetized WT mice and orexin knockout mice (KO) on arterial blood pressure (*A*), HR (*B*), Rf (*C*), and relative β-band power of EEG (*D*), an indicator of arousal. Arrowheads indicate timing of microinjection of bicuculline (20 nl). *E*: changes in above parameters expressed as area under the curve (AUC). Data are presented as means ± SE of 5 WT mice and 5 KO mice. $^{*}P < 0.05$, $^{**}P < 0.01$ vs. WT mice.

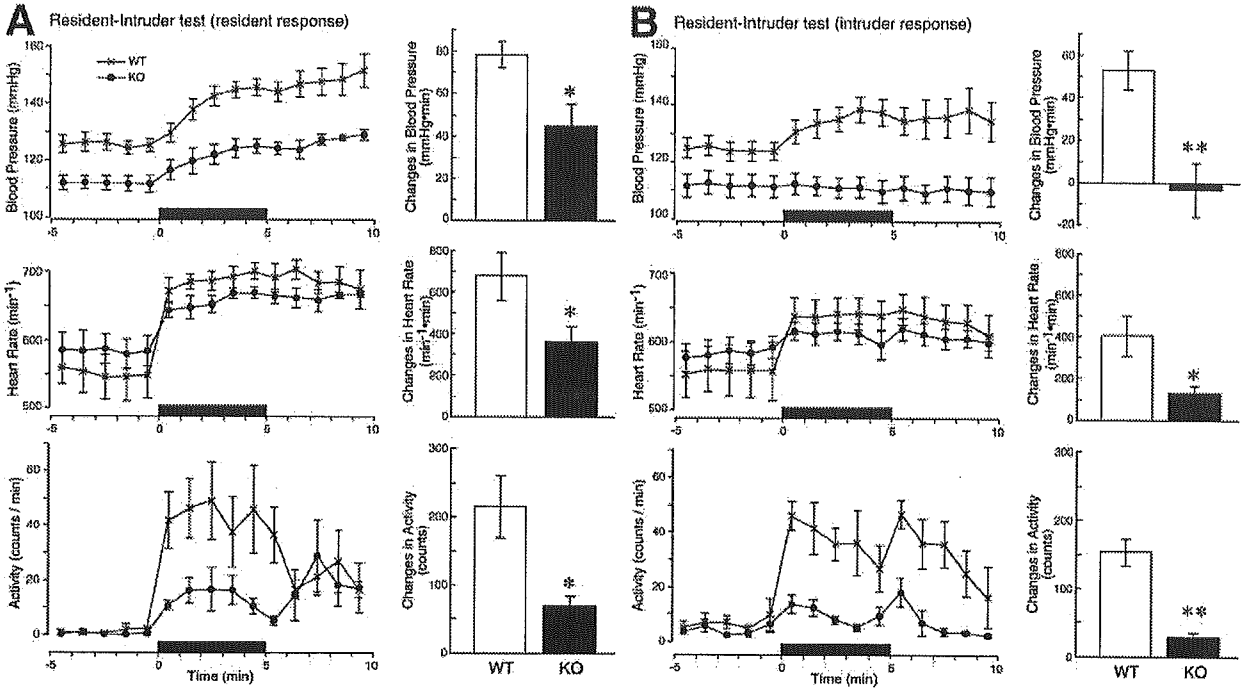

Fig. 4. Cardiovascular and behavioral responses during the resident-intruder test in radiotelemeter-indwelled freely moving WT mice and orexin KO mice. *A*: resident response when the test animal was confronted with an intruder. *B*: intruder response when the test animal intruded into a resident's home cage. The presence of an intruder (or resident) is indicated by the horizontal solid bar. Right side panels are the changes in blood pressure, HR, and activity expressed as AUC during 5 min when an intruder or resident was present in the same cage. Data are presented as means ± SE of 6 WT mice and 6 KO mice. $^{*}P < 0.05$, $^{**}P < 0.01$ vs. WT mice.

mice and wild-type mice either before or after injection of urethane (data not shown).

Experiment 4: measurement of cardiovascular parameters with indwelling catheter and pharmacological interventions. Lower basal AP in orexin knockout mice was again confirmed in this experiment (Fig. 7*A*). Basal HR of both genotypes (Fig. 7*B*) was higher than that in *experiment 3* where cardiovascular parameters were measured with radiotelemeter (Table 2). Nevertheless, there was no difference in HR between the knockout mice and wild-type mice as was the case in *experiment 3*.

To examine why basal AP was lower in orexin knockout mice, possible abnormalities of the renin-angiotensin system, vasoconstriction through vasopressin V1 receptor, or autonomic nervous system were evaluated using captopril, V1 antagonist, hexamethonium, and prazosin. Administration of captopril lowered AP in both mutant ($-12.0 \pm 1.7\%$, $n = 3$) and wild-type mice ($-11.9 \pm 2.7\%$, $n = 3$) in a similar manner ($P > 0.05$). Resultant AP was still lower in knockout mice than in wild-type mice, although the difference did not reach statistical significance presumably because of small numbers of the animals. V1 antagonist did not affect AP in either mutant ($-4.6 \pm 2.5\%$, $n = 5$) or wild-type mice ($-2.6 \pm 1.1\%$, $n = 5$). Thus resultant AP was still significantly lower in knockout mice (Fig. 7*A*). On the other hand, hexamethonium lowered AP more in wild-type ($-32.1 \pm 2.1\%$, $n = 13$) than in mutant mice ($-23.4 \pm 2.6\%$, $n = 6$; $P < 0.05$). Resulting AP was not different between the two. In a similar manner, prazosin lowered AP greater in wild-type ($-62.2 \pm 3.1\%$, $n = 5$) than in mutant mice ($-51.2 \pm 2.5\%$, $n = 5$; $P < 0.05$). Difference in AP was canceled after the treatment with prazosin (Fig. 7*A*). There was no difference in HR between the two strains with any drugs used in the current experiment (Fig. 7*B*).

Experiment 5: measurement of echocardiography. To examine the possibility that cardiac abnormality contributed to the lower AP in orexin knockout mice, we measured echocardiography in another set of the animals. Stroke volume and other basal contractile parameters were not significantly different between the two groups (Table 3).

DISCUSSION

We demonstrated here that electrical stimulation and disinhibition of GABAergic input to the perifornical area elicited the cardiovascular and respiratory defense responses and increased arousal level in urethane-anesthetized mice in a similar manner as in cats (1), rabbits (49), and rats (13, 57). A recent report that spontaneous activity of identified orexin-containing neuron in slice preparation was inhibited by the GABA-A receptor agonist muscimol supports the rele-

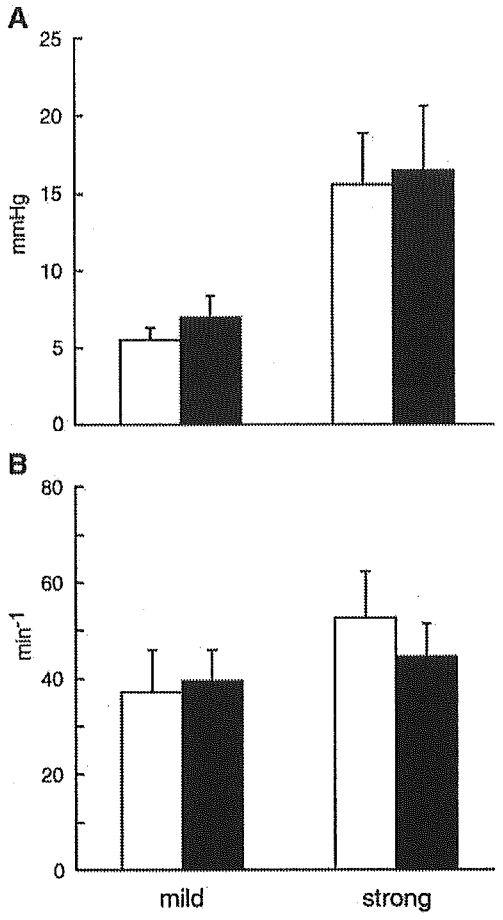

Fig. 5. Cardiovascular responses during noxious stimuli. Peak changes in blood pressure (*A*) and HR (*B*) within 30 s after the start of stimulation are summarized for WT mice (open bar, $n = 6$) and orexin KO mice (solid bar, $n = 6$). Mild and strong stimulations were applied by attaching two strengths (60 and 125 g, respectively) of vascular clamps to the tail for 10 s.

vance of our experimental setup (16, 32). The increase in AP during electrical stimulation of the hypothalamic regions seemed to be due to increasing resistance, because HR did not change much (20 beats/min, Fig. 1). It is likely that baroreflex was suppressing major increases in HR in these conditions. We did not examine the blood flow redistribution to skeletal muscle from visceral vascular beds, another characteristic of the defense response. However, mice made movement of limbs that resembled running by microinjections of bicuculline and electrical stimulations (data not shown), indicative of defense response. Cardiovascular, respiratory, and arousal components of the defense response seem to be mediated, at least in part, by orexin-containing neurons. Moreover, intrinsic orexin participates in blood pressure maintenance at basal conditions probably through activation of the sympathetic vasoconstrictor outflow. To the best of our knowledge, this is the first report demonstrating that endogenous orexins play a role in cardiovascular and respiratory regulations in the central nervous system.

Present results confirmed the proposal of possible contribution of orexin in cardiovascular regulation (3, 7, 15, 26, 36, 47, 50) and in stress-induced behavior (27, 55). In other words, our present results using knockout mice were generally in accordance with the earlier reports using exogenous application of orexin and determination of orexin content in the brain. Moreover, we successfully linked cardiovascular and stress regulatory roles of orexin by showing attenuation of defense response in orexin knockout mice in both anesthetized and freely moving conditions.

We demonstrated here diminished defense response in orexin knockout mice, but the response was not completely abolished. Preserved responses, namely short-lasting cardiorespiratory excitation at low doses of bicuculline and even similar responses in HR and Rf at high dose of bicuculline (Fig. 2), should be mediated by other transmitter(s)/modulator(s) than orexin. Existence of other factors than orexin is further suggested by incomplete disappearance of cardiovascular and behavioral responses in resident-intruder test (Fig. 4).

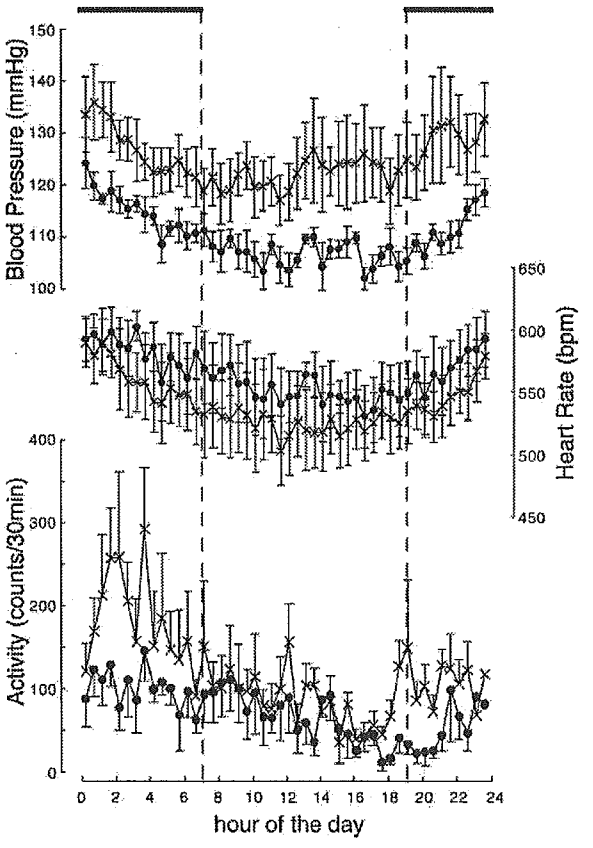

Fig. 6. Circadian patterns of blood pressure, HR, and activity. Symbols of filled circles and cross are average values from orexin KO mice ($n = 6$) and WT mice ($n = 6$), respectively. Bars indicate ±1 SE. Filled bars along the top horizontal axis indicate the dark phase of the 12:12-h light-dark cycle. bpm, Beats/min.